Metallomics

Calprotectin influences the aggregation of metal-free and metal-bound amyloid-β by direct interaction

Journal:	*Metallomics*
Manuscript ID	MT-ART-04-2018-000091.R2
Article Type:	Paper
Date Submitted by the Author:	30-Jun-2018
Complete List of Authors:	Lee, Hyuck Jin; Korea Advanced Institute of Science and Technology, Chemistry Savelieff, Masha; University of Michigan, Kang, Juhye; Ulsan National Institute of Science and Technology, Chemistry Brophy, Megan; MIT, Chemistry Nakashige, Toshiki; MIT, Chemistry Lee, Shin Jung; Ulsan National Institute of Science and Technology (UNIST), Chemistry Nolan, Elizabeth; MIT, Chemistry Lim, Mi Hee; Korea Advanced Institute of Science and Technology, Chemistry

Metallomics

PAPER

Calprotectin influences the aggregation of metal-free and metal-bound amyloid-β by direct interaction

Received 00th January 20xx,
Accepted 00th January 20xx

DOI: 10.1039/x0xx00000x

www.rsc.org/

Hyuck Jin Lee,[§a] Masha G. Savelieff,[§b] Juhye Kang,[ac] Megan Brunjes Brophy,[d] Toshiki G. Nakashige,[d] Shin Jung C. Lee,[c] Elizabeth M. Nolan*[d] and Mi Hee Lim*[a]

Proteins from the S100 family perform numerous functions and may contribute to Alzheimer's disease (AD). Herein, we report the effects of S100A8/S100A9 heterooligomer calprotectin (CP) and the S100B homodimer on metal-free and metal-bound $A\beta_{40}$ and $A\beta_{42}$ aggregation *in vitro*. Studies performed with CP-Ser [S100A8(C42S)/S100A9(C3S) oligomer] indicate that the protein influences the aggregation profile for $A\beta_{40}$ in both the absence and presence of metal ions [*i.e.*, Cu(II) and Zn(II)]. Moreover, the detection of $A\beta_{40}$–CP-Ser complexes by mass spectrometry suggests a direct interaction as a possible mechanism for the involvement of CP in $A\beta_{40}$ aggregation. Although the interaction of CP-Ser with $A\beta_{40}$ impacts $A\beta_{40}$ aggregation *in vitro*, the protein is not shown to attenuate Aβ-induced toxicity in SH-SY5Y cells. In contrast, S100B has a slight effect on the aggregation of Aβ. Overall, this work supports a potential association of CP with Aβ in the absence and presence of metal ions in AD.

Significance to Metallomics

The metallome plays a central role in many human diseases, including Alzheimer's disease (AD). Metal ion dyshomeostasis and amyloid-β (Aβ) aggregation are implicated in this debilitating neurodegenerative disorder; however, few studies have addressed interactions between transition metal ions, Aβ, and metal-binding proteins that are present in the brain. Thus, possible interactions of Cu(II) and Zn(II), two metal ions central to AD pathology, with Aβ and calprotectin (CP) and S100B were evaluated, and CP was found to noticeably affect Aβ aggregation. The results highlight that the interplay of metal ions, Aβ, and CP may have a consequence for AD pathogenesis.

Introduction

Alzheimer's disease (AD) is the most prevalent form of dementia and accounts for approximately 60% of neurodegenerative disorders.[1–10] This illness begins with mild cognitive impairment, which progresses to severe dementia and ultimately death.[7–10] Associated with these cognitive symptoms are histopathological features of AD-affected brains, notably the presence of senile plaques which primarily consist of amyloid-β (Aβ) aggregates.[3–10] Aβ is produced in the brain as a result of the proteolytic cleavage of the amyloid precursor protein (APP) by β- and γ-secretases.[6–10] A spectrum of differently sized Aβ peptides is generated, ranging from 38 to 43 amino acid residues, but the predominant forms are $A\beta_{40}$ (*ca.* 90%) and $A\beta_{42}$ (*ca.* 10%).[8–14] Both peptides tend to generate oligomeric species that have been implicated as toxic agents, and can aggregate further into mature fibrils that accumulate in senile plaques.[7–14] Although both peptides form fibrils, plaques are enriched in $A\beta_{42}$ compared to $A\beta_{40}$.[5,9,15]

Numerous chemical, biological, and biomedical research initiatives regarding AD pathogenesis have focused on Aβ; however, AD etiology remains ambiguous and other factors are almost certainly involved. This assessment is especially likely considering that therapeutics designed to principally target Aβ have failed to proceed from clinical trials into medical use,[16,17] although promising results were indicated in AD mouse models.[18,19] Therefore, current research seeks to further elucidate the etiology of AD, which may arise from multiple agents, possibly occurring in tandem and thus underlying the multifactorial nature of the disease. Along with Aβ aggregation, chronic inflammation, elevated oxidative stress, and metal ion dyshomeostasis are pervasive in the brain of AD patients and could contribute to disease onset and progression.[8–14] Since multiple parameters in addition to Aβ have been suggested to be involved in AD pathogenesis, much effort has been expended to investigate the interactions of Aβ with other agents present in the brain that may also be linked to inflammation and metal ion dyshomeostasis.[11,12,20–23] Among these candidates is the S100 protein family, members of which exhibit diverse functions, including participation in

[a]*Department of Chemistry, Korea Advanced Institute of Science and Technology (KAIST), Daejeon 34141, Republic of Korea. E-mail: miheelim@kaist.ac.kr*
[b]*SciGency Science Communications, Ann Arbor, MI 48104, USA*
[c]*Department of Chemistry, Ulsan National Institute of Science and Technology (UNIST), Ulsan 44919, Republic of Korea*
[d]*Department of Chemistry, Massachusetts Institute of Technology (MIT), Cambridge, MA 02139, USA. E-mail: lnolan@mit.edu*
[§]These authors contributed equally to this work.
Electronic Supplementary Information (ESI) available: Procedures of preparation and biochemical characterization of $S100B_{\Delta}$ and Fig. S1–S10. See DOI: 10.1039/x0xx00000x

the inflammatory response, calcium ion homeostasis, and interactions with transition metal ions.[24–29] Moreover, S100 proteins are implicated as damage-associated molecular pattern molecules (DAMPs), and are thus indicators of a sustained, chronic noninfectious inflammatory response similar to that observed in AD.[26,30,31]

S100A9 and S100B are among the most widely studied S100 proteins in AD, and both proteins have been found to be elevated in human AD brain tissue as well as AD mouse model brain tissue.[22,32–34] Knockdown of S100A9 was observed to improve memory deficits in an AD mouse model and lower plaque burden.[35] S100B ablation in AD-affected mice could similarly attenuate plaque deposition in specific brain regions,[36] whereas S100B overexpression in the AD mouse model exacerbated plaque deposition and AD pathology.[37] These studies support possible roles for S100A9 and S100B in AD pathogenesis.

Calprotectin (CP), a heterooligomer of S100A8 and S100A9 that chelates transition metal ions and participates in the metal-withholding innate immune response,[38] is relatively understudied in AD research. An *in vitro* study demonstrated that S100A9 could promote Aβ fibrillization,[21] and *ex vivo* analysis of postmortem AD tissue exhibited elevated levels of aggregated S100A9, possibly co-localized with Aβ, but not S100A8 and thus not CP.[22,32,34] Nevertheless, this observation does not preclude the possibility that CP and Aβ interact. Recently, there has been growing consensus that structured Aβ oligomers are relatively more toxic than Aβ fibrils, and a biomolecule that does not aggravate Aβ fibrillization could still exhibit toxicity in AD *via* structured soluble oligomers.[39–42]. Therefore, CP was selected as a case study and possible S100 protein candidate that may not exacerbate Aβ fibrillization since it was not found to be co-aggregated and increased in AD plaques but may influence Aβ aggregation. The effect of S100B, another metal-binding S100 protein that exists in the brain,[43–45] on Aβ aggregation was also investigated.

Herein, we report the impact of CP and S100B on the formation of (i) Aβ fibrils and (ii) Aβ oligomers, as well as (iii) the relative distribution of various-sized peptide species of both metal-free and metal-associated Aβ (metal–Aβ). In addition, we demonstrate that CP directly interacts with Aβ by employing electrospray ionization mass spectrometry (ESI-MS). We further establish that the combined presence of both Aβ and CP is not able to improve Aβ-triggered toxicity in human neuroblastoma SH-SY5Y (5Y) cells, suggesting that the interaction of Aβ and CP does not attenuate Aβ-induced cytotoxicity. Although the distribution of S100A8 and S100A9 has been determined in AD mouse model brain tissue,[33] to the best of our knowledge, this study is the first report on the influence of CP on the behavior (*e.g.*, aggregation and toxicity) of both $A\beta_{40}$ and $A\beta_{42}$ in the absence and presence of metal ions.

Results and discussion

Selection and preparation of S100 proteins

All apo S100 proteins employed in this work were obtained by recombinant expression in *Escherichia coli*.[29,46] CP variants were purified as apo heterodimers. The 24-kDa CP heterodimer exhibits two transition-metal-binding sites at the S100A8/S100A9 interface. Site 1 is a His_3Asp motif comprised of (A8)His83, (A8)His87, (A9)His20, and (A9)Asp30. Site 2 is a His_6 site comprised of (A8)His17, (A8)His27, (A9)His91, (A9)His95, (A9)His103, and (A9)His105. Both of these sites coordinate Cu(II) and Zn(II) with high affinity.[29,46] In this work, we employed two CP variants, CP-Ser and CP-$Ser_{\Delta\Delta}$, that were biochemically evaluated.[29] Each S100 subunit of CP contains one Cys residue, and CP-Ser is the S100A8(C42S)/S100A9(C3S) variant. Neither Cys residue is in close proximity to the metal-binding sites, and CP-Ser has been used extensively in order to avoid the use of reducing agents or the formation of disulfide bonds during metal-binding studies.[29] CP-$Ser_{\Delta\Delta}$ harbors eight additional point mutations (His/Asp → Ala) and cannot bind transition metal ions at the His_3Asp and His_6 sites. This protein allowed us to investigate whether the metal-binding capacity of CP influences its interactions with Aβ in the absence and presence of metal ions.

The 21-kDa S100B homodimer also contains two transition-metal-binding sites, which are located at the homodimer interface. At pH 6.5, these sites are defined by His15 and His25 from one monomer, and His85 and Glu89 from the other monomer.[47,48] Both of these sites coordinate Zn(II) and Cu(II).[47] In this work, we employed S100B and the $S100B_{\Delta}$ variant, which lacks the metal-binding sites (Supporting Information and Fig. S1, ESI†).

Influence of CP-Ser on the formation of β-sheet-rich Aβ aggregates with and without metal Ions

The generation of β-sheet-rich aggregates of metal-free Aβ (prepared in Chelex-treated buffer) and metal–Aβ [0.1 or 1.0 equiv of Zn(II) or Cu(II) relative to Aβ] in the absence and presence of CP-Ser and CP-$Ser_{\Delta\Delta}$ was monitored by the thioflavin-T (ThT) assay and transmission electron microscopy (TEM) (Fig. 1 and 2 and Fig. S2–S4, ESI†). We first investigated the effect of these proteins on the aggregation of $A\beta_{40}$. Under metal-free conditions, incubation of $A\beta_{40}$ with CP-Ser or CP-$Ser_{\Delta\Delta}$ led to lower fluorescent responses from ThT than the sample containing $A\beta_{40}$ only. ThT becomes fluorescent upon binding to β-sheet-rich aggregates, and its fluorescence intensity is a quantifiable measure of the amount of β-sheet-rich structures present.[49] Upon treatment of $A\beta_{40}$ with CP-Ser or CP-$Ser_{\Delta\Delta}$, a decrease in fluorescence intensity greater than 80% was observed (Fig. 1b). In addition, the aggregation kinetics of $A\beta_{40}$ with and without CP-Ser were monitored by the ThT assay (Fig. S2, ESI†). The elongation phase of $A\beta_{40}$ aggregation with and without CP-Ser occurred from the beginning of the incubation and reached a plateau after *ca*. 8 h. The fluorescence intensity of ThT in the samples containing CP-Ser and $A\beta_{40}$ was *ca*. 20% of that observed for the samples of $A\beta_{40}$ without CP-Ser after 24 h incubation. This indicates that the formation of a smaller amount of β-sheet-rich $A\beta_{40}$ aggregates upon treatment of CP-Ser. Moreover, CP-Ser was

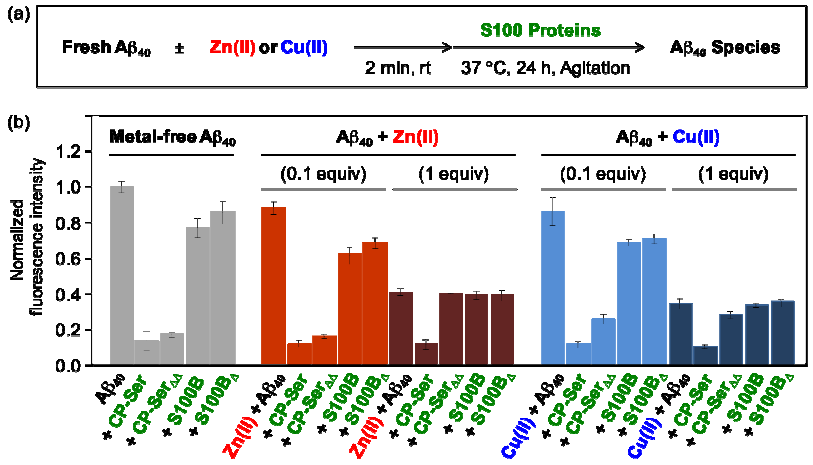

Fig. 1 Effects of S100 proteins (CP-Ser, CP-Ser$_{\Delta\Delta}$, S100B, and S100B$_{\Delta}$) on the aggregation of metal-free Aβ_{40} and metal–Aβ_{40}. (a) Scheme of the experiment. (b) Analysis of the degree of forming β-sheet-rich Aβ_{40} aggregates, observed by the ThT assay, on Aβ_{40} samples with S100 proteins following 24 h incubation. Conditions: [Aβ_{40}] = 20 μM; [$ZnCl_2$ or $CuCl_2$] = 2 or 20 μM; [S100 proteins] = 20 μM; pH 7.4 (for metal-free and Zn(II) experiments) or pH 6.6 (for Cu(II) experiments); 24 h incubation; 37 °C.

indicated to delay the aggregation kinetics of Aβ_{40} following the incubation time up to 24 h (Fig. S2, ESI†). Together, CP-Ser was observed to modulate the aggregation of Aβ_{40}.

In the presence of metal ions [*i.e.*, Zn(II) and Cu(II)], the ThT assay indicated that both CP-Ser and CP-Ser$_{\Delta\Delta}$ could influence metal–Aβ fibrillization depending on the equivalents of metal present. CP-Ser reduced the formation of β-sheet-rich Aβ_{40} aggregates with 1 and 2 equiv of Zn(II) relative to the protein (concentrations of Aβ and CP are equivalent), whereas this protein did not affect aggregation when > 2 equiv of Zn(II) were added (Fig. 1b and Fig. S3b, ESI†). On the other hand, CP-Ser$_{\Delta\Delta}$ may have some influence at sub-stoichiometric levels of Zn(II), but may not have a significant effect on Aβ_{40} aggregation at supra-stoichiometric Zn(II) (Fig. 1b and Fig. S3b, ESI†). Similar trends were observed upon the addition of Cu(II) to CP-Ser, showing alteration of Aβ_{40} aggregate formation with up to 1 equiv of Cu(II). In contrast, CP-Ser$_{\Delta\Delta}$ exhibited a marginal effect on Cu(II)–Aβ_{40} aggregation (Fig. 1b). These results suggest that the presence of CP-Ser or CP-Ser$_{\Delta\Delta}$ reduces the formation of β-sheet-rich (ThT-reactive) Aβ aggregates.[50]

The results from the ThT assay, indicative of the formation of fewer β-sheet-rich Aβ_{40} aggregates in the presence of CP-Ser and CP-Ser$_{\Delta\Delta}$, were corroborated by TEM studies that demonstrated the generation of proportionally more amorphous species for Aβ_{40} incubated with either CP-Ser or CP-Ser$_{\Delta\Delta}$, compared to the sample with Aβ_{40} only (Fig. 2a). Although CP is reported to form amyloid at low pH,[51] under our experimental conditions, smaller and shorter aggregates of both CP-Ser and CP-Ser$_{\Delta\Delta}$ were detected and could be readily distinguished from aggregated Aβ species (Fig. 2a). In the presence of Zn(II) and Cu(II), spherical as well as small aggregates of CP-Ser were observed (Fig. 2a). Moreover, TEM revealed a lesser effect of CP-Ser$_{\Delta\Delta}$, relative to CP-Ser, on metal–Aβ_{40} fibrillization (Fig. 2a).

The ability of CP-Ser to alter Aβ_{40} aggregation at stoichiometric Zn(II) or Cu(II) (Fig. 1b) compared to CP-Ser$_{\Delta\Delta}$, which had no influence against Aβ_{40} fibrillization under these conditions, indicates that the metal-binding sites of CP, and hence metal chelation, contribute to the modification of metal–Aβ_{40} aggregation. The effect of both CP-Ser and CP-Ser$_{\Delta\Delta}$ to impact metal-free Aβ_{40}, which likely adopts distinct structural conformations to metal–Aβ_{40},[52–57] also highlights the importance of protein-protein interactions and structures on the ability of proteins to alter Aβ aggregation, in addition to metal chelation.

Apparent dissociation constant (K_d) values obtained by fluorescence methods have been reported for both CP and Aβ for metal ions. Although these experiments have been performed under different conditions, a comparison of these available K_d values suggests that CP-Ser can disrupt metal binding to Aβ. For instance, the two Zn(II) sites of the CP heterodimer are reported to bind Zn(II) at pH 7.5 with K_d values of 133 pM and 185 nM, by the site 1 and site 2, respectively.[58] Recently, CP was reported to bind Cu ion with K_d values of 0.2 pM and 4 pM at pH 7.0, respectively, by the site 1 and site 2.[59] On the other hand, reported K_d values obtained by fluorescence measurements were varied for Aβ (for Zn(II), from 1 to 300 μM; for Cu(II), *ca.* 0.1 nM).[60–65] Note that metal binding affinities of Aβ have been shown to be dependent on the technique employed (*e.g.*, isothermal titration calorimetric analysis, UV-vis spectroscopy, and nuclear magnetic resonance spectroscopy) and experimental conditions (*e.g.*, concentrations, temperature, and buffer) [for example, *ca.* 1–20 μM for Zn(II) and 0.4–70 nM for Cu(II)].[64–72] Thus, regardless of the method of analysis and experimental conditions, the data from previous studies indicate that CP-Ser binds Zn(II) and Cu(II) with higher affinities than Aβ.[58–72]

To probe whether CP-Ser interferes with metal binding to Aβ, competition experiments were performed between Aβ_{40},

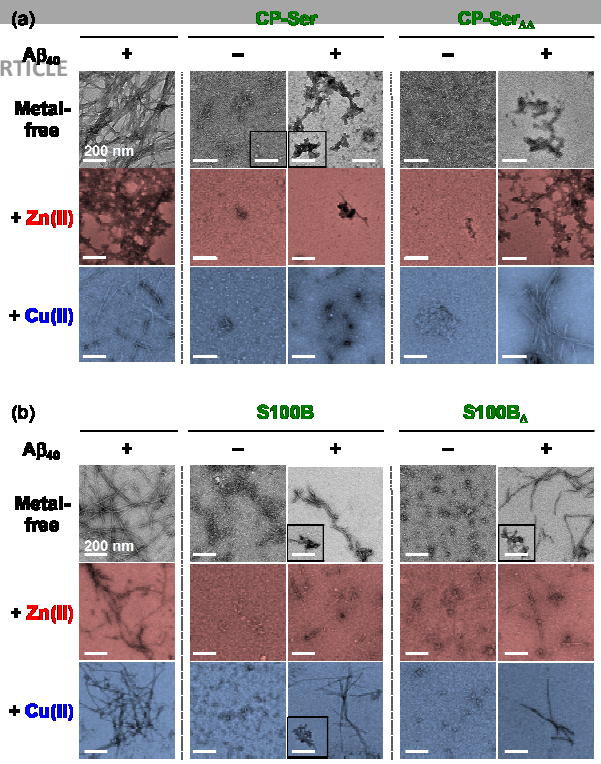

Fig. 2 Morphologies of S100 proteins and the resultant $A\beta_{40}$ aggregates with or without S100 proteins and metal ions, monitored by TEM. $A\beta_{40}$ aggregates were generated by 24 h treatment with or without (a) [CP-Ser and CP-Ser$_{\Delta\Delta}$] or (b) [S100B and S100B$_{\Delta}$] in the absence and presence of metal ions (1 equiv). The inset images represent minor species. Conditions: [$A\beta_{40}$] = 20 μM; [$ZnCl_2$ or $CuCl_2$] = 20 μM; [S100 proteins] = 20 μM; pH 7.4 (for metal-free and Zn(II) experiments) or pH 6.6 (for Cu(II) experiments); 24 h incubation; 37 °C; constant agitation. Scale bar = 200 nm.

CP-Ser, and Cu(II) by ESI-MS. Either $A\beta_{40}$ mixed with Cu(II) initially followed by CP-Ser, or CP-Ser mixed with Cu(II) first followed by $A\beta_{40}$, Cu(II)-bound $A\beta_{40}$ was not shown (Fig. S5, ESI†). The detection of Cu(II)–$A\beta_{40}$ complexes in the control sample of $A\beta_{40}$ treated with Cu(II) confirmed that complexes could be observed under our experimental conditions. Thus, the absence of Cu(II)–$A\beta_{40}$ in the presence of CP-Ser suggests that Cu(II) binding of $A\beta_{40}$ can be interfered by CP-Ser.

Next, we evaluated the effect of CP-Ser and CP-Ser$_{\Delta\Delta}$ on $A\beta_{42}$ aggregation. In contrast to the $A\beta_{40}$ aggregation studies, neither CP-Ser nor CP-Ser$_{\Delta\Delta}$ modulated the aggregation of $A\beta_{42}$ with and without metal ions (Fig. S4b and c, ESI†). Although $A\beta_{40}$ and $A\beta_{42}$ differ by only two C-terminal amino acids, these residues have profound effects on Aβ aggregation kinetics, species distribution (*e.g.*, monomers and oligomers), and the structural conformations of aggregates in the absence and presence of metal ions.[52–57] It is possible that the distinct interactions of CP-Ser and CP-Ser$_{\Delta\Delta}$ with $A\beta_{40}$ and $A\beta_{42}$ *via* direct protein-protein interactions (*vide infra*, ESI-MS analysis, Fig. 4) may differ as a result of the distinct conformations of $A\beta_{40}$ and $A\beta_{42}$ species,[52–55] which could affect $A\beta_{40}$ and $A\beta_{42}$ aggregation to different extents.

Effect of S100B on metal-free and metal-induced Aβ aggregation

Examination of how S100B and S100B$_{\Delta}$ affect Aβ aggregation revealed the behavior that differs from CP-Ser and CP-Ser$_{\Delta\Delta}$. Under metal-free conditions, initial inspection by the ThT assay indicated that S100B and S100B$_{\Delta}$ could slightly influence metal-free $A\beta_{40}$ aggregation because a small attenuation of ThT fluorescence occurred (Fig. 1b). The TEM studies also demonstrated that S100B and S100B$_{\Delta}$ could induce small and subtle morphological changes in metal-free $A\beta_{40}$ fibrillization, resulting in the formation of shorter metal-free $A\beta_{40}$ fibrils with few amorphous aggregates, compared to the sample of $A\beta_{40}$ only (Fig. 2b). As the morphologies of both S100B and S100B$_{\Delta}$ aggregates were noticeably different from Aβ aggregates, we could distinguish accumulated Aβ and S100B/S100B$_{\Delta}$ species (Fig. 2b). The truncated fibrils that form in the presence of S100B, relative to the broader and longer fibrils in the samples of $A\beta_{40}$ only, bind fewer ThT molecules and hence generate a slightly lower fluorescence signal in the ThT assay (Fig. 1b). Since fibrils are still formed, the fluorescence signal is not as effectively abrogated as observed for CP-Ser with $A\beta_{40}$.

In the presence of metal ions, a similar pattern emerged as for CP-Ser and CP-Ser$_{\Delta\Delta}$ at sub-stoichiometric levels of metal ions. At 0.1 equiv of Zn(II) or Cu(II), the ThT assay indicated that both S100B and S100B$_{\Delta}$ had a small, but measurable influence on the amount of β-sheet-rich $A\beta_{40}$ aggregates formed (Fig. 1b). On the other hand, the ThT assay with 1 equiv of Zn(II) or Cu(II) indicated that neither S100B nor S100B$_{\Delta}$ could significantly alter the production of β-sheet-rich $A\beta_{40}$ aggregates (Fig. 1b). These results were supported by TEM at 1 equiv of Zn(II) or Cu(II), which presented relatively small-sized fibrils, instead of larger and longer fibrils, that were distinct from S100B and S100B$_{\Delta}$ aggregates (Fig. 2b). Although S100B binds transition metal ions, including Cu(II) and Zn(II),[45,47,48,73] the protein may not be able to tune the aggregation of metal–$A\beta_{40}$. Similar to CP-Ser and CP-Ser$_{\Delta\Delta}$, neither S100B nor S100B$_{\Delta}$ could interfere with fibrillization of metal-free $A\beta_{42}$ and metal–$A\beta_{42}$ (Fig. S4b and d, ESI†). Overall, S100B and S100B$_{\Delta}$ were not observed to affect metal-free and metal-bound $A\beta_{40}$ aggregation like CP.

Size distributions of metal-free $A\beta_{40}$ and metal–$A\beta_{40}$ aggregates generated upon treatment with S100 proteins

To assess the impact of these four S100 proteins on $A\beta_{40}$ oligomer formation, gel/Western blot and dot blot analysis were performed to visualize the molecular weight (MW) distribution of $A\beta_{40}$ species upon incubation of $A\beta_{40}$ with each S100 protein (Fig. 3a and b and Fig. S6 and S7, ESI†). An anti-$A\beta_{40}$ antibody (6E10)[74,75] was employed to visualize $A\beta_{40}$, an anti-S100A9 antibody was used to detect CP-Ser and CP-Ser$_{\Delta\Delta}$, and Coomassie blue staining was employed to indicate S100B and S100B$_{\Delta}$. Gel electrophoresis was conducted in running buffer containing 1% SDS to mobilize protein samples through the gel matrix. This amount of SDS likely disrupts complexes of S100 proteins with $A\beta_{40}$ that may exist, but does not break-up SDS-resistant $A\beta_{40}$ oligomers. Therefore, the bands observed in the 6E10 blots can be ascribed solely to $A\beta_{40}$ oligomers (Fig. 3a

and Fig. S6 and S7, ESI†; gray), and this assignment is further supported by the anti-S100A9 blots and Coomassie blue stains since these data present almost identical patterns of S100 proteins in the absence and presence of $A\beta_{40}$ (Fig. 3a and Fig.

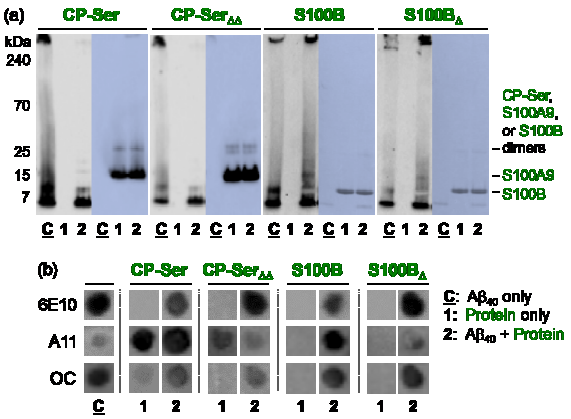

Fig. 3 Analyses of the resultant metal-free $A\beta_{40}$ species upon treatment with S100 proteins (CP-Ser, CP-Ser$_{\Delta\Delta}$, S100B, and S100B$_{\Delta}$). (a) $A\beta_{40}$ species produced after 24 h incubation with or without the proteins, visualized by gel/Western blot using an anti-Aβ antibody (6E10; gray gels) or an anti-S100A9 antibody (blue gels; CP-Ser and CP-Ser$_{\Delta\Delta}$) as well as Coomassie blue staining (blue gels; S100B and S100B$_{\Delta}$). (b) Dot blot analysis of metal-free $A\beta_{40}$ species generated after 24 h incubation with or without the proteins, monitored employing an anti-Aβ antibody (6E10), an anti-amyloid oligomer antibody (A11), and an anti-amyloid fibril antibody (OC). Samples: (Control, C) $A\beta_{40}$; (1) S100 proteins; (2) $A\beta_{40}$ + S100 proteins. Conditions: [$A\beta_{40}$] = 20 μM; [S100 proteins] = 20 μM; pH 7.4; 24 h incubation; 37 °C.

S6 and S7 ESI†; blue). Clear bands representing monomeric S100A9 (*ca*. 13 kDa) and S100B (*ca.* 11 kDa) as well as the CP-Ser heterodimer (*ca.* 24 kDa) and the S100B homodimer (*ca.* 21 kDa) were observed.

Without metal ions, addition of CP-Ser to $A\beta_{40}$ resulted in smaller oligomers compared to the oligomers in the samples containing $A\beta_{40}$ only (Fig. 3a). This observation is in general agreement with the observations from the ThT assays and TEM (Fig. 1b and 2a), which together indicates that CP-Ser modulates the aggregation pathway of $A\beta_{40}$. To obtain further insight into this process, the $A\beta_{40}$ oligomers and fibrils formed upon incubation with CP-Ser were detected by dot blots using the amyloid-oligomer targeting antibody (A11)[76,77] and a fibril-reactive antibody (OC)[78] (Fig. 3b). The intensity of the dots blotted with A11 were similar between samples of CP-Ser alone and CP-Ser with $A\beta_{40}$. In contrast, both CP-Ser alone and CP-Ser with $A\beta_{40}$ had low reactivity against OC (presented lower intensity than $A\beta_{40}$ only). These results suggested that CP-Ser formed structured amyloid oligomers, but not fibrils, under our experimental conditions. Fibril formation of $A\beta_{40}$ begins with a nucleation phase in which soluble $A\beta_{40}$ monomers produce small oligomers that seed the generation of protofibrils in the elongation phase.[42] CP-Ser, either as a heterodimer or higher-order oligomer, might interfere with the ability of $A\beta_{40}$ oligomers to form a nucleus for fibrillization, potentially by forming complexes with $A\beta_{40}$. Indeed, the anti-S100A9 blots (Fig. 3a) show a slight streaking pattern in the presence of 1% SDS, which may be evidence for formation of an $A\beta_{40}$–CP-Ser complex.

CP-Ser$_{\Delta\Delta}$ also impacted the MW distribution of $A\beta_{40}$ species (Fig. 3a and b). Dot blots showed that CP-Ser$_{\Delta\Delta}$ also responded to the A11 antibody, but not to the OC antibody (Fig. 3b), indicating no significance of the metal-binding sites in the formation of CP-Ser oligomers. Nevertheless, CP-Ser$_{\Delta\Delta}$ appeared to oligomerize or bind to $A\beta_{40}$ less than CP-Ser as evidenced by the absence of streaking in the anti-S100A9 blot (Fig. 3a).

Both S100B and S100B$_{\Delta}$ exhibited a relatively subtle effect on the formation of $A\beta_{40}$ oligomers. In the gel/Western blot with 6E10, both S100B and S100B$_{\Delta}$ with $A\beta_{40}$ exhibited smearing bands, compared to the samples of $A\beta_{40}$ only (Fig. 3a). This impact on the generation of $A\beta_{40}$ oligomers was also confirmed by the dot blot where A11-treated dots were more intense in the presence of S100B and S100B$_{\Delta}$ than in the absence of the protein, especially for S100B. Moreover, the intensities of the dots blotted with the OC antibody for the samples of $A\beta_{40}$ and S100B or S100B$_{\Delta}$ were similar to the sample of $A\beta_{40}$ only. This observation is in agreement with both the ThT (Fig. 1b) and TEM analyses (Fig. 2b) presenting only a slightly discernible influence on $A\beta_{40}$ fibril formation, which may not be resolvable by gel/Western and dot blots. The samples containing only S100B and S100B$_{\Delta}$ did not react to the A11 antibody, which could indicate that structured amyloid oligomers were not produced upon incubation with these proteins under our experimental conditions and may be one contributing factor for the distinct behavior of CP-Ser and CP-Ser$_{\Delta\Delta}$ versus S100B and S100B$_{\Delta}$ towards $A\beta_{40}$ aggregation.

The size distribution of $A\beta_{40}$ and S100 protein aggregates with different amounts of metal ions [*i.e.*, 0.1 and 1.0 equiv of Zn(II) and Cu(II)] upon incubation was also investigated by gel/Western blot (Fig. S6 and S7, ESI†). The results generally agree with the data collected employing other methods (Fig. 1b and 2). One exception was the lack of change in $A\beta_{40}$ oligomer distribution, observed by gel/Western blot, when CP-Ser$_{\Delta\Delta}$ was added to the samples containing Zn(II) (0.1 equiv). This observation contrasted the results from ThT and TEM that showed an influence of CP-Ser$_{\Delta\Delta}$ on Aβ fibril formation at sub-stoichiometric amounts of metal ions (Fig. 1b). This apparent discrepancy may be explained by the production of larger $A\beta_{40}$ aggregates in the presence of CP-Ser$_{\Delta\Delta}$, which are incapable of passing into the gel matrix and may be observed as a high intensity at the top of the gel within the well. Alternatively, the 1% SDS may dissociate the oligomeric forms of CP-Ser$_{\Delta\Delta}$ in the presence of metal ions under our experimental conditions (Fig. S6 and S7, ESI†). Another possible explanation could be that CP-Ser$_{\Delta\Delta}$ oligomers influence the population of metal-free $A\beta_{40}$, when sub-stoichiometric metal ions were added, but might leave metal–$A\beta_{40}$ species unaffected, which appeared in the gel as metal–$A\beta_{40}$ samples without CP-Ser$_{\Delta\Delta}$.

With S100B or S100B$_{\Delta}$ at 1 equiv of Zn(II) or Cu(II) to $A\beta_{40}$, new bands were observed by gel/Western blot (Fig. S6, ESI†). In the presence of Cu(II), S100B and S100B$_{\Delta}$ exhibited multiple

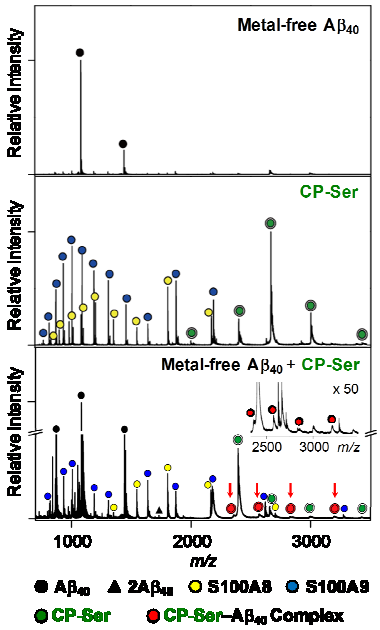

Fig. 4 ESI-MS studies for monitoring the formation of $A\beta_{40}$–CP-Ser complexes in the absence of metal ions. The MS spectra of metal-free $A\beta_{40}$ (top), CP-Ser (middle), and metal-free $A\beta_{40}$ treated with CP-Ser (bottom) indicate protein peaks, including subunits of CP-Ser (S100A8 and S100A9), metal-free $A\beta_{40}$, and CP-Ser–$A\beta_{40}$ complexes. In the bottom panel, the *m/z* values from 2,300 to 3,500 are zoomed in to present the $A\beta_{40}$–CP-Ser complexes (inset). Conditions (final concentrations): [$A\beta_{40}$] = 5 μM; [CP-Ser] = 5 μM; pH 7.5; 24 h incubation; 37 °C; constant agitation.

bands which correspond to the MW of the S100B homodimer (Fig. S6b and S7b, ESI†). S100B contains Cys residues, and these dimeric species may be generated by disulfide bond formation between S100B monomers, as a previous study suggested.[73] These bands may also indicate that both S100B and $S100B_{\Delta}$ can interact with $A\beta_{40}$ and metal ions; however, these proteins may not have a significant effect on the aggregation or fibrillization of $A\beta_{40}$ as indicated by the ThT assay (Fig. 1b) and TEM (Fig. 2b).

Interaction between CP-Ser or S100B and $A\beta_{40}$ identified by ESI-MS

Because CP-Ser exhibited a pronounced effect on $A\beta_{40}$ aggregation, we undertook further studies to determine whether a direct interaction between CP-Ser and $A\beta_{40}$ could be observed in the form of complexes by ESI-MS. Mass spectra of the samples containing CP-Ser only and mixtures of CP-Ser and $A\beta_{40}$ revealed the expected peaks attributable to the CP-Ser heterodimer (green) as well as monomers of S100A8 (yellow circles) and S100A9 (blue circles) (Fig. 4). The spectra obtained for CP-Ser and $A\beta_{40}$ also contained peaks assigned to monomeric and dimeric $A\beta_{40}$ (black circles and triangles, respectively), as well as peaks assigned to $A\beta_{40}$–CP-Ser complexes (red circles) (Fig. 4). In addition to complex formation, the charge distributions of the CP-Ser peaks were altered in the presence of $A\beta_{40}$, which may be triggered by the interactions between the two proteins (Fig. 4). Moreover, in the case of S100B, complex formation between S100B and $A\beta_{40}$ was not observed under our experimental conditions (Fig. S8, ESI†), supporting a weaker interaction between the two proteins, as observed by the ThT assay (Fig. 1b) and TEM experiment (Fig. 2b). Overall, the direct interaction between CP-Ser and $A\beta_{40}$ was observed, suggesting a connection between such protein-protein interaction and the ability of CP-Ser to generate less β-sheet-rich aggregates of $A\beta_{40}$.

Cytotoxicity associated with CP-Ser in the absence and presence of $A\beta_{40}$ and metal ions

Although cells secrete CP to protect themselves from pathogen invasion, elevated and uncontrolled levels of CP may have detrimental effects.[30] To assess this possibility in the context of the current work, the viability of human neuroblastoma SH-SY5Y (5Y) cells treated with CP-Ser was examined (Fig. 5a). CP-Ser was pre-incubated for 8 h in either the absence or presence of Aβ and applied to 5Y cells. After a 6 h incubation with 5Y cells, the CP-Ser species, pre-incubated in the absence of Aβ, did not cause noticeable toxicity, whereas a 24 h incubation afforded some toxicity (*ca*. 20% cell death) (Fig. 5a). Dot blots with the A11 antibody indicated that, in the presence of 5Y cells, CP-Ser formed structured oligomers at the 6 h time point, and that more A11-detectable species were observed at the longer, 24 h time point (Fig. 5b). In contrast, structured oligomers were not detected with the A11 antibody when the protein was incubated alone without cells in buffered solution for 8 h (Fig. S9, ESI†) indicating either that the CP-Ser did not aggregate or that it aggregated into amorphous aggregates unreactive to A11 antibody. These structured oligomeric species of CP-Ser may cause the observed toxicity.

CP-Ser combined with $A\beta_{40}$ could generate slightly more toxic species than CP-Ser or $A\beta_{40}$ alone (Fig. 5a). For instance, *ca.* 69% cell survival was observed after 6 h incubation with CP-Ser and $A\beta_{40}$ compared to 96% and 83% cell survival for cell treated with CP-Ser or $A\beta_{40}$ alone. These trends were also observed after 24 h incubation (Fig. 5a). When combined together in cell culture, CP-Ser and $A\beta_{40}$ formed structured oligomeric species, detected by A11 (Fig. 5b), and these A11-reactive aggregates may exhibit cytotoxicity (Fig. 5a).

In the case of $A\beta_{42}$, similar cytotoxicity was observed for the pre-incubated CP-Ser and $A\beta_{42}$ mixture and $A\beta_{42}$ alone after a 6 h incubation (*ca.* 77% cell viability; Fig. 5a). In the presence of added Zn(II) and Cu(II), greater than *ca*. 96% of cells survived upon 6 h incubation with pre-incubated (for 8 h) CP-Ser (Fig. S10, ESI†). Moreover, Zn(II)-treated CP-Ser showed no toxicity at the 24 h time point (*ca.* 100% cell survival), whereas CP-Ser with Cu(II) showed some toxicity (*ca*. 86% cell viability) (Fig. S10, ESI†). The cell viability of CP-Ser with metal ions and Aβ was relatively similar to that from the cells treated with metal ions and Aβ. Therefore, CP-Ser may not be able to affect the toxicity induced by metal-associated Aβ species significantly.

Overall, CP-Ser species may be toxic agents to cells exposed to the proteins longer than 24 h, either *via* the formation of A11-reactive structured oligomers or because they may sequester metal ions from the media since exogenous Zn(II) or Cu(II) mitigates toxicity. Additionally, the toxicity of CP-Ser species at 24 h could be slightly increased by interacting with $A\beta_{40}$ in the absence of metal ions. Based on these cell studies, CP-Ser may not have significant influence on the toxicity induced by $A\beta_{40}$ or $A\beta_{42}$, with and without metal ions. Further studies are required to understand the toxicity caused by CP-Ser and CP-Ser–Aβ.

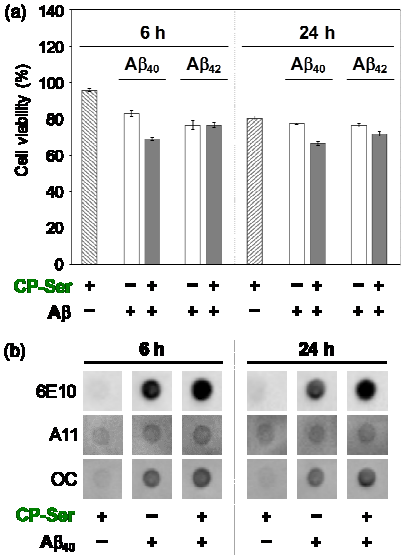

Fig. 5 Determination of the toxicity of CP-Ser with and without Aβ in cells and their conformational state by dot blot. (a) Viability of 5Y cells incubated with CP-Ser and/or Aβ. CP-Ser was pre-incubated in both the absence and presence of Aβ for 8 h and incubated with 5Y cells for 6 (left) or 24 h (right). Cytotoxicity was measured by the MTT assay. The viability values were calculated by comparison to cells treated with a volume of H_2O equal to the protein added. Error bars represent the standard error from three independent experiments. Conditions (final concentrations): [CP-Ser] = 5 μM; [Aβ] = 5 μM. (b) Dot blot assay of pre-incubated (for 8 h) CP-Ser with and without $A\beta_{40}$ after 6 (left) or 24 h (right) incubation with cells. Conditions: [CP-Ser] = 5 μM; [$A\beta_{40}$] = 5 μM.

Conclusions

In this work, we examined the ability of CP-Ser and S100B to alter both metal-free Aβ and metal–Aβ aggregation. Out of the proteins examined, the influence of CP-Ser on $A\beta_{40}$ aggregation was most pronounced. Such an impact on $A\beta_{40}$ aggregation in the absence and presence of metal ions could potentially occur by the generation of complexes between CP-Ser and $A\beta_{40}$ as observed by ESI-MS, or by the formation of CP-Ser oligomers that might alter the aggregation of $A\beta_{40}$ and enhance the toxicity triggered by $A\beta_{40}$.

The molecular details of how CP-Ser inhibits metal-free $A\beta_{40}$ and metal–$A\beta_{40}$ fibril formation are unknown. One possibility suggested by this work is that CP-Ser interacts directly with metal-free $A\beta_{40}$ to alter $A\beta_{40}$ aggregation, possibly *via* direct protein-protein interactions as supported by ESI-MS. Another potential mechanism is that CP-Ser influences metal–$A\beta_{40}$ aggregation by disrupting metal binding to $A\beta_{40}$, which is supported by the observation that CP-$Ser_{\Delta\Delta}$, which lacks defined metal binding sites, indicated no influence on Aβ aggregation when ≥ 1 equiv of Zn(II) and Cu(II) were added under the assay conditions. Therefore, the impact of CP-Ser could be dual in nature, by directly interacting with $A\beta_{40}$ to limit aggregation and by interfering metal binding to $A\beta_{40}$ to attenuate metal-induced $A\beta_{40}$ aggregation, which was revealed by comparing the behavior of CP-Ser to CP-$Ser_{\Delta\Delta}$.

By demonstrating the interplay between CP-Ser and Aβ, our studies suggest that CP and Aβ may interact *in vivo*. If indeed the case, this work also supports the increasingly appreciated multi-faceted nature of AD pathology, wherein several factors may be involved in the progression of the disease.[79–81] In closing, protein-protein networks should be identified to gain a better understanding of AD pathogenesis.

Experimental

Materials and methods

All reagents were purchased from commercial suppliers and used as received unless otherwise stated. CP-Ser and S100B proteins were overexpressed, purified, and characterized as previously reported.[29,46] Trace metal contamination was removed from buffers and solutions used for Aβ experiments by treating with Chelex (Sigma-Aldrich, St. Louis, MO, USA). $A\beta_{40}$ (DAEFRHDSGYEVHHQKLVFFAEDVGSNKGAIIGLMVGGVV) and $A\beta_{42}$ (DAEFRHDSGYEVHHQKLVFFAEDVGSNKGAIIGLMVGG-VVIA) were purchased from Anaspec (Fremont, CA, USA). We have carried out the experiments with more than three replicates with at least two different batches of Aβ. All double distilled H_2O (ddH_2O) used during experiments was obtained from a Milli-Q Direct 16 system (Merck KGaA, Darmstadt, Germany). TEM images were recorded on a Philips CM-100 transmission electron microscope [Microscopy and Image Analysis Laboratory (MIL), University of Michigan, Ann Arbor, MI, USA] or a JEOL JEM-2100 transmission electron microscope [UNIST Central Research Facilities (UCRF), Ulsan, Republic of Korea]. A SpectraMax M5 microplate reader (Molecular Devices, Sunnyvale, CA, USA) was used to measure the fluorescence intensity and absorbance for the assays.

Protein preparation and purification

The S100A8 and S100A9 subunits for CP-Ser and CP-$Ser_{\Delta\Delta}$ were overexpressed in *Escherichia coli* BL21 (DE3), and the proteins were reconstituted, purified, and stored at −80 °C according to previously established methods.[29] The procedure gives the apo heterodimers. Each protein sample was freeze-thawed only once before use. S100B was overexpressed in *Escherichia coli* BL21 (DE3) and purified as previously described.[46] Procedures

for the expression and purification of $S100B_{\Delta}$ are provided as Supporting Information.

Aβ aggregation experiments

All experiments with Aβ were performed according to previously published methods.[74,75,82–84] Aβ peptides were dissolved in ammonium hydroxide (NH_4OH, 1% v/v, aq), aliquoted, lyophilized, and stored at −80 °C. A stock solution (*ca*. 200 μM) was prepared by dissolving Aβ in NH_4OH (1% w/v, aq, 10 μL) followed by dilution with ddH_2O, as reported previously.[74,75,82–84] The $A\beta_{40}$ concentration was determined by measuring the absorbance of the solution at 280 nm (ε = 1450 $M^{-1}cm^{-1}$ for $A\beta_{40}$; ε = 1490 $M^{-1}cm^{-1}$ for $A\beta_{42}$). HEPES [4-(2-hydroxyethyl)-1-piperazineethanesulfonic acid; 20 mM], pH 7.4 (for metal-free and Zn(II) samples) and pH 6.6 (for Cu(II) samples), 150 mM NaCl was used for the studies. For the experiments, freshly dissolved Aβ (20 μM) in the absence and presence of a metal chloride salt ($ZnCl_2$ or $CuCl_2$; 20 μM) was treated with S100 proteins (20 μM) and incubated for 24 h at 37 °C with constant agitation.

ThT assay

The amount of Aβ fibrillization and the kinetics of $A\beta_{40}$ aggregation upon treatment of CP-Ser were investigated as previously described.[23,85–87] (i) For measuring the amount of β-sheet-rich Aβ aggregates, each Aβ sample (20 μM) with or without metal ions ($ZnCl_2$ or $CuCl_2$; 2 or 20 μM) and S100 proteins (CP-Ser, $CP\text{-}Ser_{\Delta\Delta}$, S100B, and $S100B_{\Delta}$; 20 μM) was obtained after 24 h incubation at 37 °C with constant agitation and diluted with buffer [20 mM HEPES, pH 7.4 (for metal-free and Zn(II) experiments) or pH 6.6 (for Cu(II) experiments), 150 mM NaCl]. (ii) For monitoring $A\beta_{40}$ aggregation kinetics, each Aβ sample (20 μM) with or without CP-Ser was obtained after 0, 0.3, 0.6, 1, 2, 4, 8, 12, and 24 h incubation at 37 °C with constant agitation. The samples were incubated for 20 min with ThT (20 μM) and the fluorescence intensity was measured by a microplate reader (λ_{ex} = 440 nm; λ_{em} = 490 nm) and normalized relative to that of metal-free Aβ aggregates (without CP-Ser) generated by 24 h incubation.

Gel electrophoresis with Western blot

The Aβ peptide experiments described above were analyzed by gel electrophoresis with two different visualization methods: (i) Western blotting (gel/Western blot) with two different antibodies [anti-Aβ antibody (6E10; Covance, Princeton, NJ, USA) or anti-S100A9 antibody (Santa Cruz Biotechnology, Dallas, TX, USA)];[74,75,82–84] (ii) Coomassie blue staining. Each sample from the experiments was separated using a 10–20% gradient Tris-tricine gel (Thermo Fisher, Grand Island, NY, USA). First, the CP-Ser samples were separated on the gel, transferred to a nitrocellulose membrane, and blocked for 3 h at room temperature with a bovine serum albumin (BSA) solution (3% w/v) in Tris-buffered saline (TBS, Fisher, Pittsburgh, PA, USA) containing 0.1% Tween-20 (Sigma-Aldrich; TBS-T). The membrane was treated with the Aβ monoclonal antibody (6E10, 1:2,000, BSA 2% w/v, in TBS-T) or anti-S100A9 antibody (1:1000, BSA 2% w/v, in TBS-T) overnight at 4 °C and then probed with a horseradish peroxidase conjugated goat anti-mouse secondary antibody (1:5,000; Cayman Chemical, Ann Arbor, MI, USA) or donkey anti-goat secondary antibody (1:5,000; Jackson ImmunoResearch Laboratories, West Grove, PA, USA) in 2% w/v BSA (in TBS-T) solution for 1 h at room temperature against anti-Aβ and anti-S100A9, respectively. The protein bands were visualized using Thermo Scientific Supersignal West Pico Chemiluminescent Substrate (Rockford, IL, USA) or a homemade ECL kit[88] was used to visualize the results on a ChemiDoc MP Imaging System (Bio-rad, Hercules, CA, USA).

The gels run with S100B- and $S100B_{\Delta}$-containing samples were stained with Coomassie blue for 30 min and destained for 3 h. Gel images were obtained by a ChemiDoc MP system (Bio-rad). Then, the dye was completely destained from the gel, and the gel was transferred to a nitrocellulose membrane for Western blot with 6E10 (1:2,000) in a solution of 2% w/v BSA (in TBS-T) and a horseradish peroxidase conjugated goat anti-mouse secondary antibody (1:5,000) same as the Western blot for the CP-Ser samples.

Dot blot assay

Solutions of protein aggregates (2 μL) from the experiments were spotted on a nitrocellulose membrane and the membrane was blocked with BSA solution (3% w/v; RMBIO, Missoula, MT, USA) in Tris-buffered saline containing 0.01% Tween 20 (TBS-T) at room temperature for 1.5 h. Then, the membrane was incubated with a primary antibody, 6E10 (1:2,000), A11 (1:2,500; Millipore, Billerica, MA, USA) or OC (1:2,500; Millipore) in a solution of 2% w/v BSA (in TBS-T) for 1.5 h at room temperature. After washing with TBS-T three times (7 min each), the horseradish peroxidase-conjugated goat anti-mouse (for 6E10) or goat anti-rabbit (for A11 and OC) secondary antibody (1:5,000; Cayman Chemical Company for 6E10, 1:2,500; Promega for A11 and OC) in the solution of BSA (2% w/v in TBS-T) was added to the membrane and incubated for 1 h at room temperature. A homemade ECL kit[88] was used to visualize the results on a ChemiDoc MP Imaging System (Bio-rad). The same membrane was stripped by treating with hydrogen peroxide (H_2O_2) for 30 min at room temperature, washed 4 times with TBS-T for 10 min each, blocked with the solution of BSA (3% w/v in TBS-T), and incubated with the primary antibodies (6E10, A11, and OC) as described above.

Transmission electron microscopy (TEM)

Protein samples for TEM measurements were prepared following previously reported methods.[74,75,82–84] Glow discharged grids (Formvar/Carbon 300-mesh, Electron Microscopy Sciences, Hatfield, PA, USA) were treated with samples from the experiments (5 μL) for 2 min at room temperature. Excess sample was removed with filter paper and the grids were washed with ddH_2O three times. Each grid was stained with uranyl acetate (1% w/v ddH_2O; 5 μL) for 1 min. Uranyl acetate was blotted off and grids were dried for at least 20 min at room temperature. Images of samples were

taken by a Philips CM-100 transmission electron microscope (80 kV, 25,000× magnification; MIL, University of Michigan, Ann Arbor, MI, USA) or JEOL JEM-2100 transmission electron microscope (200 kV, 25,000× magnification; UCRF, Ulsan, Republic of Korea).

Mass spectrometric studies

Mass spectrometric experiments with CP-Ser and $A\beta_{40}$ were performed on a Synapt G2-Si Q-ToF mass spectrometer equipped with electrospray ionization (ESI) source (Waters, Manchester, UK). $A\beta_{40}$ (20 μM) was mixed with CP-Ser (20 μM) or S100B (20 μM) in 10 mM ammonium acetate (pH 7.5). The prepared samples were incubated at 37 °C for 24 h without agitation. Incubated samples were diluted 4-fold with 10 mM ammonium acetate (pH 7.5) before injection, and the final concentration of peptides was adjusted to 5 μM. The capillary voltage, sampling cone voltage, and source temperature were adjusted to 2.8 kV, 70 V, and 40 °C, respectively, for CP-Ser and 1.8 kV, 40 V, and 40 °C, respectively, for S100B. Moreover, for the competition experiments, the samples were prepared in 10 mM ammonium acetate (pH 7.5) through two different addition orders of $A\beta_{40}$, $CuCl_2$, and CP-Ser: (i) $A\beta_{40}$ (20 μM) was first treated with $CuCl_2$ (20 μM) followed by addition of CP-Ser (20 μM); (ii) CP-Ser (20 μM) was first incubated with $CuCl_2$ followed by treatment with $A\beta_{40}$. The prepared samples were incubated at 37 °C for 1 h without agitation, and then were diluted by four fold with 10 mM ammonium acetate (pH 7.5) (the final concentration of peptides was adjusted to 5 μM) before injection to the mass spectrometer. The capillary voltage, sampling cone voltage, and source temperature were adjusted to 1.8 kV, 40 V, and 40 °C, respectively. As the resolution of the instrument was not high enough to determine the monoisotopic masses for CP-Ser subunits, heterodimeric CP-Ser, or homodimeric S100B complexes with $A\beta_{40}$, all peaks were assigned using the *m/z* values of the most abundant isotopes. For example, if the *m/z* of an apex isotope is divided by the mass of the proteins and the result is an integer, the peak can be assigned as one charge state of the proteins.

Cell viability measurements

The SH-SY5Y (5Y) cell line was purchased from the American Type Culture Collection (ATCC, Manassas, VA, USA). The cell line was maintained in media containing 50% minimum essential medium (MEM) and 50% F12 (GIBCO), and supplemented with 10% fetal bovine serum (Sigma-Aldrich), and 100 U/mL penicillin (GIBCO). Cells were grown and maintained at 37 °C in a humidified atmosphere with 5% CO_2. The cell culture used in this work did not indicate mycoplasma contamination. Cell viability upon treatment with CP-Ser was determined by the MTT assay [MTT = 3-(4,5-dimethylthiazol-2-yl)-2,5-diphenyltetrazolium bromide]. Cells were seeded in a 96 well plate (13,000 cells in 100 μL per well). Cells were treated with pre-incubated proteins for 8 h with and without metal ions at 37 °C with constant agitation. After 6 or 24 h incubation with cells, MTT [25 μL of 5 mg/mL in PBS (pH 7.4, GIBCO)] was added to each well, and the plate was incubated for 4 h at 37 °C. Formazan produced by cells was solubilized using an acidic solution of *N*,*N*-dimethylformamide (DMF, pH 4.5, 50% v/v, aq) and sodium dodecyl sulfate (SDS, 20% w/v) overnight at room temperature in the dark. The absorbance was measured at 600 nm by a microplate reader. Cell viability was calculated relative to cells containing a volume of H_2O equal to the volume of protein added.

Conflicts of interest

There are no conflicts to declare.

Acknowledgements

This work was supported by the National Research Foundation of Korea (NRF) grant funded by the Korean government (NRF-2017R1A2B3002585 and NRF-2016R1A5A1009405) and Korea Advanced Institute of Science and Technology (KAIST) (to M.H.L.); National Science Foundation (NSF) (CHE-1352132) (to E.M.N.). J.K. acknowledges the Global Ph.D. fellowship program through the NRF funded by the Ministry of Education (NRF-2015HIA2A1030823). T.G.N. is a recipient of a NSF Graduate Research Fellowship. The MIT Biophysical Instrumentation Facility for the Study of Complex Macromolecular Systems is supported by NSF grant 0070319.

References

1 Alzheimer's Association. 2017 Alzheimer's disease facts and figures. *Alzheimers Dement.*, 2017, **13**, 325–373.
2 M. W. Beck, A. S. Pithadia, A. S. DeToma, K. J. Korshavn and M. H. Lim, Ligand design to target and modulate metal–protein interactions in neurodegenerative diseases in *Ligand Design in Medicinal Inorganic Chemistry*, ed. T. Storr, John Wiley & Sons, Ltd, NY, 2014, Ch. 10, pp257–286.
3 H. J. Lee, K. J. Korshavn, A. Kochi, J. S. Derrick and M. H. Lim, Cholesterol and metal ions in Alzheimer's disease, *Chem. Soc. Rev.*, 2014, **43**, 6672–6682.
4 A. S. Pithadia and M. H. Lim, Metal-associated amyloid-β species in Alzheimer's disease, *Curr. Opin. Chem. Biol.*, 2012, **16**, 67–73.
5 A. Rauk, The chemistry of Alzheimer's disease, *Chem. Soc. Rev.*, 2009, **38**, 2698–2715.
6 P. Faller, Copper and zinc binding to amyloid-β: coordination, dynamics, aggregation, reactivity and metal-ion transfer, *ChemBioChem*, 2009, **10**, 2837–2845.
7 J. S. Derrick and M. H. Lim, Tools of the trade: investigations into design strategies of small molecules to target components in Alzheimer's disease, *ChemBioChem*, 2015, **16**, 887–898.
8 R. Jakob-Roetne and H. Jacobsen, Alzheimer's disease: from pathology to therapeutic approaches, *Angew. Chem. Int. Ed.*, 2009, **48**, 3030–3059.
9 A. S. DeToma, S. Salamekh, A. Ramamoorthy and M. H. Lim, Misfolded proteins in Alzheimer's disease and type II diabetes, *Chem. Soc. Rev.*, 2012, **41**, 608–621.
10 M. G. Savelieff, S. Lee, Y. Liu and M. H. Lim, Untangling amyloid-β, tau, and metals in Alzheimer's disease, *ACS Chem. Biol.*, 2013, **8**, 856–865.
11 K. P. Kepp, Bioinorganic chemistry of Alzheimer's disease, *Chem. Rev.*, 2012, **112**, 5193–5239.

12 C. Rodríguez-Rodríguez, M. Telpoukhovskaia and C. Orvig, The art of building multifunctional metal-binding agents from basic molecular scaffolds for the potential application in neurodegenerative diseases, *Coord. Chem. Rev.*, 2012, **256**, 2308–2332.

13 I. W. Hamley, The amyloid beta peptide: a chemist's perspective. Role in Alzheimer's and fibrillization, *Chem. Rev.*, 2012, **112**, 5147–5192.

14 C. Haass and D. J. Selkoe, Soluble protein oligomers in neurodegeneration: lessons from the Alzheimer's amyloid β-peptide, *Nat. Rev. Mol. Cell Biol.*, 2007, **8**, 101–112.

15 L. Gu and Z. Guo, Alzheimer's $A\beta_{42}$ and $A\beta_{40}$ peptides form interlaced amyloid fibrils, *J. Neurochem.*, 2013, **126**, 305–311.

16 A. Abbott and E. Dolgin, Leading Alzheimer's theory survives drug failure, *Nature*, 2016, **540**, 15–16.

17 F. Panza, D. Seripa, V. Solfrizzi, B. P. Imbimbo, M. Lozupone, A. Leo, R. Sardone, G. Gagliardi, L. Lofano, B. C. Creanza, P. Bisceglia, A. Daniele, A. Bellomo, A. Greco and G. Logroscino, Emerging drugs to reduce abnormal β-amyloid protein in Alzheimer's disease patients, *Expert Opin. Emerg. Drugs*, 2016, **21**, 377–391.

18 R. B. DeMattos, K. R. Bales, D. J. Cummins, J.-C. Dodart, S. M. Paul and D. M. Holtzman, Peripheral anti-Aβ antibody alters CNS and plasma Aβ clearance and decreases brain Aβ burden in a mouse model of Alzheimer's disease, *Proc. Natl. Acad. Sci. U. S. A.*, 2001, **98**, 8850–8855.

19 J.-C. Dodart, K. R. Bales, K. S. Gannon, S. J. Greene, R. B. DeMattos, C. Mathis, C. A. DeLong, S. Wu, X. Wu, D. M. Holtzman and S. M. Paul, Immunization reverses memory deficits without reducing brain Aβ burden in Alzheimer's disease model, *Nat. Neurosci.*, 2002, **5**, 452–457.

20 J. Milojevic and G. Melacini, Stoichiometry and affinity of the human serum albumin-Alzheimer's Aβ peptide interactions, *Biophys. J.*, 2011, **100**, 183–192.

21 C. Zhang, Y. Liu, J. Gilthorpe and J. R. C. van der Maarel, MRP14 (S100A9) protein interacts with Alzheimer beta-amyloid peptide and induces its fibrillization, *PLoS One*, 2012, **7**, e32953.

22 C. E. Shepherd, J. Goyette, V. Utter, F. Rahimi, Z, Yang, C. L. Geczy and G. M. Halliday, Inflammatory S100A9 and S100A12 proteins in Alzheimer's disease, *Neurobiol. Aging*, 2006, **27**, 1554–1563.

23 T. S. Choi, H. J. Lee, J. Y. Han, M. H. Lim and H. I. Kim, Molecular insights into human serum albumin as a receptor of amyloid-β in the extracellular region, *J. Am. Chem. Soc.*, 2017, **139**, 15437–15445.

24 I. P. Korndörfer, F. Brueckner and A. Skerra, The crystal structure of the human $(S100A8/S100A9)_2$ heterotetramer, calprotectin, illustrates how conformational changes of interacting α-helices can determine specific association of two EF-hand proteins, *J. Mol. Biol.*, 2007, **370**, 887–898.

25 D. Benet Bosco Dhas, B. Vishnu Bhat and D. Bahubali Gane, Role of calprotectin in infection and inflammation, *Curr. Pediatr. Res.*, 2012, **16**, 83–94.

26 I. A. Clark and B. Vissel, Amyloid β: one of three danger-associated molecules that are secondary inducers of the proinflammatory cytokines that mediate Alzheimer's disease, *Br. J. Pharmacol.*, 2015, **172**, 3714–3727.

27 J. A. Hayden, M. B. Brophy, L. S. Cunden and E. M. Nolan, High-affinity manganese coordination by human calprotectin is calcium-dependent and requires the histidine-rich site formed at the dimer interface, *J. Am. Chem. Soc.*, 2013, **135**, 775–787.

28 R. Donato, B. R. Cannon, G. Sorci, F. Riuzzi, K. Hsu, D. J. Weber and C. L. Geczy, Functions of S100 proteins, *Curr. Mol. Med.*, 2013, **13**, 24–57.

29 M. B. Brophy, J. A. Hayden and E. M. Nolan, Calcium ion gradients modulate the zinc affinity and antibacterial activity of human calprotectin, *J. Am. Chem. Soc.*, 2012, **134**, 18089–18100.

30 A. Schiopu and O. S. Cotoi, S100A8 and S100A9: DAMPs at the crossroads between innate immunity, traditional risk factors, and cardiovascular disease, *Mediators Inflamm.*, 2013, **2013**, 828354.

31 C. Venegas and M. T. Heneka, Danger-associated molecular patterns in Alzheimer's disease, *J. Leukoc. Biol.*, 2017, **101**, 87–98.

32 H. Akiyama, K. Ikeda, M. Katoh, E. G. McGeer and P. L. McGeer, Expression of MRP14, 27E10, interferon-α and leukocyte common antigen by reactive microglia in postmortem human brain tissue, *J. Neuroimmunol.*, 1994, **50**, 195–201.

33 M. P. Kummer, T. Vogl, D. Axt, A. Griep, A. Vieira-Saecker, F. Jessen, E. Gelpi, J. Roth and M. T. Heneka, MRP14 deficiency ameliorates amyloid β burden by increasing microglial phagocytosis and modulation of amyloid precursor protein processing. *J. Neurosci.*, 2012, **32**, 17824–17829.

34 C. Wang, A. G. Klechikov, A. L. Gharibyan, S. K. T. S. Wärmländer, J. Jarvet, L. Zhao, X. Jia, S. K. Shankar, A. Olofsson, T. Brännström, Y. Mu, A. Gräslund and L. A. Morozova-Roche, The role of pro-inflammatory S100A9 in Alzheimer's disease amyloid-neuroinflammatory cascade, *Acta Neuropathol.*, 2014, **127**, 507–522.

35 T.-Y. Ha, K.-A. Chang, J. A. Kim, H.-S. Kim, S. Kim, Y. H. Chong, Y.-H. Suh, S100A9 knockdown decreases the memory impairment and the neuropathology in Tg2576 mice, AD animal model, *PLoS One*, 2010, **5**, e8840.

36 E. Roltsch, L. Holcomb, K. A. Young, A. Marks and D. B. Zimmer, PSAPP mice exhibit regionally selective reductions in gliosis and plaque deposition in response to S100B ablation, *J. Neuroinflamm.*, 2010, **7**, 78.

37 T. Mori, N. Koyama, G. W. Arendash, Y. Horikoshi-Sakuraba, J. Tan and T. Town, Overexpression of human S100B exacerbates cerebral amyloidosis and gliosis in the Tg2576 mouse model of Alzheimer's disease, *Glia*, 2010, **58**, 300–314.

38 E. M. Zygiel and E. M. Nolan, Transition metal sequestration by the host-defense protein calprotectin, *Annu. Rev. Biochem.*, 2018, *In press*.

39 S. T. Ferreira, M. V. Lourenco, M. M. Oliveira and F. G. De Felice, Soluble amyloid-β oligomers as synaptotoxins leading to cognitive impairment in Alzheimer's disease, *Front. Cell. Neurosci.*, 2015, **9**, 191.

40 K. L. Viola and W. L. Klein, Amyloid β oligomers in Alzheimer's disease pathogenesis, treatment, and diagnosis, *Acta Neuropathol.*, 2015, **129**, 183–206.

41 U. Sengupta, A. N. Nilson and R. Kayed, The role of amyloid-β oligomers in toxicity, propagation, and immunotherapy, *EBioMedicine*, 2016, **6**, 42–49.

42 S. J. C. Lee, E. Nam, H. J. Lee, M. G. Savelieff and M. H. Lim, Towards an understanding of amyloid-β oligomers: characterization, toxicity mechanisms, and inhibitors, *Chem. Soc. Rev.*, 2017, **46**, 310–323.

43 C. W. Heizmann, Ca^{2+}-binding S100 proteins in the central nervous system, *Neurochem. Res.*, 1999, **24**, 1097–1100.

44 S. C. Tiu, W. Y. Chan, C. W. Heizmann, B. W. Schäfer, S. Y. Shu and D. T. Yew, Differential expression of S100B and S100A6 in the human fetal and aged cerebral cortex, *Dev. Brain Res.*, 2000, **119**, 159–168.

45 B. A. Gilston, E. P. Skaar and W. J. Chazin, Binding of transition metals to S100 proteins, *Sci. China Life Sci.*, 2016, **59**, 792–801.

46 M. B. Brophy, T. G. Nakashige, A. Gaillard and E. M. Nolan, Contributions of the S100A9 C-terminal tail to high-affinity

Mn(II) chelation by the host-defense protein human calprotectin, *J. Am. Chem. Soc.*, 2013, **135**, 17804–17817.
47 S. Z. Senior, L. L. Mans, H. D. VanGuilder, K. A. Kelly, M. P. Hendrich and T. E. Elgren, Catecholase activity associated with Copper-S100B, *Biochemistry*, 2003, **42**, 4392–4397.
48 T. Ostendorp, J. Diez, C. W. Heizmann and G. Fritz, The crystal structures of human S100B in the zinc- and calcium-loaded state at three pH values reveal zinc ligand swapping, *Biochim. Biophys. Acta*, 2011, **1813**, 1083–1091.
49 M. R. Nilsson, Techniques to study amyloid fibril formation *in vitro*, *Methods*, 2004, **34**, 151–160.
50 H. LeVine 3rd, Thioflavine T interaction with synthetic Alzheimer's disease β-amyloid peptides: detection of amyloid aggregation in solution, *Protein Sci.*, 1993, **2**, 404–410.
51 K. Yanamandra, O. Alexeyev, V. Zamotin, V. Srivastava, A. Shchukarev, A.-C. Brorsson, G. G, Tartaglia, T. Vogl, R. Kayed, G. Wingsle, J. Olsson, C. M. Dobson, A. Bergh, F. Elgh and L. A. Morozova-Roche, Amyloid formation by the pro-inflammatory S100A8/A9 proteins in the ageing prostate. *PLoS One*, 2009, **4**, e5562.
52 N. J. Economou, M. J. Giammona, T. D. Do, X. Zheng, D. B. Teplow, S. K. Buratto and M. T. Bowers, Amyloid β⍰protein assembly and Alzheimer's disease: Dodecamers of Aβ42, but not of Aβ40, seed fibril formation, *J. Am. Chem. Soc.*, 2016, **138**, 1772–1775.
53 R. Roychaudhuri, M. Yang, A. Deshpande, G. M. Cole, S. Frautschy, A. Lomakin, G. B. Benedek and D. B. Teplow, C-terminal turn stability determines assembly differences between Aβ40 and Aβ42, *J. Mol. Biol.*, 2013, **425**, 292–308.
54 S. L. Bernstein, N. F. Dupuis, N. D. Lazo, T. Wyttenbach, M. M. Condron, G. Bitan, D. B. Teplow, J.-E. Shea, B. T. Ruotolo, C. V. Robinson and M. T. Bowers, Amyloid-β protein oligomerization and the importance of tetramers and dodecamers in the aetiology of Alzheimer's disease, *Nat. Chem.*, 2009, **1**, 326–331.
55 G. Bitan, M. D. Kirkitadze, A. Lomakin, S. S. Vollers, G. B. Benedek and D. B. Teplow, Amyloid β-protein (Aβ) assembly: Aβ40 and Aβ42 oligomerize through distinct pathways, *Proc. Natl. Acad. Sci. U. S. A.*, 2003, **100**, 330–335.
56 T. M. Ryan, N. Kirby, H. D. T. Mertens, B. Roberts, K. J. Barnham, R. Cappai, C. L. L. Pham, C. L. Masters and C. C. Curtain, Small angle X-ray scattering analysis of Cu^{2+}-induced oligomers of the Alzheimer's amyloid β peptide, *Metallomics*, 2015, **7**, 536–543.
57 J. T. Pedersen, J. Østergaard, N. Rozlosnik, B. Gammelgaard and N. H. H. Heegaard, Cu(II) mediates kinetically distinct, non-amyloidogenic aggregation of amyloid-β peptides, *J. Biol. Chem.*, 2011, **286**, 26952–26963.
58 M. B. Brophy, J. A. Hayden and E. M. Nolan, Calcium ion gradients modulate the zinc affinity and antibacterial activity of human calprotectin, *J. Am. Chem. Soc.*, 2012, **134**, 18089–18100.
59 A. N. Besold, B. A. Gilston, J. N. Radin, C. Ramsoomair, E. M. Culbertson, C. X. Li, B. P. Cormack, W. J. Chazin, T. E. Kehl-Fie and V. C. Culotta, Role of calprotectin in withholding zinc and copper from *Candida albicans*, *Infect. Immun.*, 2018, **86**, e00779.
60 T. R. Young, A. Kirchner, A. G. Wedd and Z. Xiao, An integrated study of the affinities of the Aβ16 peptide for Cu(I) and Cu(II): implications for the catalytic production of reactive oxygen species, *Metallomics*, 2014, **6**, 505–517.
61 B. Alies, E. Renaglia, M. Rózga, W. Bal and P. Faller, Cu(II) affinity for the Alzheimer's peptide: tyrosine fluorescence studies revisited, *Anal. Chem.*, 2013, **85**, 1501–1508.
62 V. Tõugu, A. Karafin and P. Palumaa, Binding of zinc(II) and copper(II) to the full-length Alzheimer's amyloid-β peptide, *J. Neurochem.*, 2008, **104**, 1249–1259.
63 W. Garzon-Rodriguez, A. K. Yatsimirsky and C. G. Glabe, Binding of Zn(II), Cu(II), and Fe(II) ions to Alzheimer's Aβ peptide studied by fluorescence, *Bioorg. Med. Chem. Lett.*, 1999, **9**, 2243–2248.
64 J. Danielsson, R. Pierattelli, L. Banci and A. Gräslund, High-resolution NMR studies of the zinc-binding site of the Alzheimer's amyloid β-peptide, *FEBS J.*, 2007, **274**, 46–59.
65 C. Talmard, A. Bouzan and P. Faller, Zinc binding to amyloid-β: Isothermal titration calorimetry and Zn competition experiments with Zn sensors, *Biochemistry*, 2007, **46**, 13658–13666.
66 I. Zawisza, M. Rózga and W. Bal, Affinity of copper and zinc ions to proteins and peptides related to neurodegenerative conditions (Aβ, APP, α-synuclein, PrP), *Coord. Chem. Rev.*, 2012, **256**, 2297–2307.
67 J. Guo, W. Sun and F. Liu, Brazilin inhibits the Zn^{2+}-mediated aggregation of amyloid β-protein and alleviates cytotoxicity, *J. Inorg. Biochem.*, 2017, **177**, 183–189.
68 S. Noël, S. B. Rodriguez, S. Sayen, E. Guillon, P. Faller and C. Hureau, Use of a new water-soluble Zn sensor to determine Zn affinity for the amyloid-β peptide and relevant mutants, *Metallomics*, 2014, **6**, 1220–1222.
69 L. Hong, T. M. Carducci, W. D. Bush, C. G. Dudzik, G. L. Millhauser and J. D. Simon, Quantification of the binding properties of Cu^{2+} to the amyloid beta peptide: Coordination spheres for human and rat peptides and implication on Cu^{2+}-induced aggregation, *J. Phys. Chem. B*, 2010, **114**, 11261–11271.
70 L. Q. Hatcher, L. Hong, W. D. Bush, T. Carducci and J. D. Simon, Quantification of the binding constant of copper(II) to the amyloid-beta peptide, *J. Phys. Chem. B*, 2008, **112**, 8160–8164.
71 L. Hong, W. D. Bush, L. Q. Hatcher and J. Simon, Determining thermodynamic parameters from isothermal calorimetric isotherms of the binding of macromolecules to metal cations originally chelated by a weak ligand, *J. Phys. Chem. B*, 2008, **112**, 604–611.
72 L. Guilloreau, L. Damian, Y. Coppel, H. Mazarguil, M. Winterhalter and P. Faller, Structural and thermodynamical properties of Cu^{II} amyloid-β16/28 complexes associated with Alzheimer's disease, *J. Biol. Inorg. Chem.*, 2006, **11**, 1024–1038.
73 I. S. M. Lee, M. Suzuki, N. Hayashi, J. Hu, L. J. Van Eldink, K. Titani and M. Nishikimi, Copper-dependent formation of disulfide-linked dimer of S100B protein, *Archiv. Biochem. Biophys.*, 2000, **374**, 137–141.
74 M. W. Beck, S. B. Oh, R. A. Kerr, H. J. Lee, S. H. Kim, S. Kim, M. Jang, B. T. Ruotolo, J.-Y. Lee and M. H. Lim, A rationally designed small molecule for identifying an *in vivo* link between metal–amyloid-β complexes and the pathogenesis of Alzheimer's disease, *Chem. Sci.*, 2015, **6**, 1879–1886.
75 H. J. Lee, K. J. Korshavn, Y. Nam, J. Kang, T. J. Paul, R. A. Kerr, I. S. Youn, M. Ozbil, K. S. Kim, B. T. Ruotolo, R. Prabhakar, A. Ramamoorthy and M. H. Lim, Structural and mechanistic insights into development of chemical tools to control individual and inter-related pathological features in Alzheimer's disease, *Chem. Eur. J.*, 2017, **23**, 2706–2715.
76 R. Kayed, E. Head, J. L. Thompson, T. M. McIntire, S. C. Milton, C. W. Cotman and C. G. Glabe, Common structure of soluble amyloid oligomers implies common mechanism of pathogenesis, *Science*, 2003, **300**, 486–489.
77 C. G. Glabe, Structural classification of toxic amyloid oligomers, *J. Biol. Chem.*, 2008, **283**, 29639–29643.
78 R. Kayed, E. Head, F. Sarsoza, T. Saing, C. W. Cotman, M. Necula, L. Margol, J. Wu, L. Breydo, J. L. Thompson, S. Rasool, T. Gurlo, P. Butler and C. G. Glabe, Fibril specific, conformation dependent antibodies recognize a generic epitope common to amyloid fibrils and fibrillar oligomers

that is absent in prefibrillar oligomers, *Mol. Neurodegener.*, 2007, **2**, 18.
79 K. Herrup, The case for rejecting the amyloid cascade hypothesis, *Nat. Neurosci.*, 2015, **18**, 794–799.
80 E. S. Musiek and D. M. Holtzman, Three dimensions of the amyloid hypothesis: time, space and 'wingmen', *Nat. Neurosci.*, 2015, **18**, 800–806.
81 M. C. Carreiras, E. Mendes, M. J. Perry, A. P. Francisco and J. Marco-Contelles, The multifactorial nature of Alzheimer's disease for developing potential therapeutics, *Curr. Top. Med. Chem.*, 2013, **13**, 1745–1770.
82 S. Lee, X. Zheng, J. Krishnamoorthy, M. G. Savelieff, H. M. Park, J. R. Brender, J. H. Kim, J. S. Derrick, A. Kochi, H. J. Lee, C. Kim, A. Ramamoorthy, M. T. Bowers and M. H. Lim, Rational design of a structural framework with potential use to develop chemical reagents that target and modulate multiple facets of Alzheimer's disease, *J. Am. Chem. Soc.*, 2014, **136**, 299–310.
83 J. S. Derrick, R. A. Kerr, Y. Nam, S. B. Oh, H. J. Lee, K. G. Earnest, N. Suh, K. L. Peck, M. Ozbil, K. J. Korshavn, A. Ramamoorthy, R. Prabhakar, E. J. Merino, J. Shearer, J.-Y. Lee, B. T. Ruotolo and M. H. Lim, A redox-active, compact molecule for cross-linking amyloidogenic peptides into nontoxic, off-pathway aggregates: *in vitro* and *in vivo* efficacy and molecular mechanisms, *J. Am. Chem. Soc.*, 2015, **137**, 14785–14797.
84 J. Kang, S. J. C. Lee, J. S. Nam, H. J. Lee, M.-G. Kang, K. J. Korshavn, H.-T. Kim, J. Cho, A. Ramamoorthy, H.-W. Rhee, T.-H. Kwon and M. H. Lim, An iridium(III) complex as a photoactivatable tool for oxidation of amyloidogenic peptides with subsequent modulation of peptide aggregation, *Chem. Eur. J.*, 2017, **23**, 1645–1653.
85 H. F. Stanyon and J. H. Viles, Human serum albumin can regulate amyloid-β peptide fiber growth in the brain interstitium, *J. Biol. Chem.*, 2012, **287**, 28163–28168.
86 K. Rajasekhar, S. N. Suresh, R. Manjithaya and T. Govindaraju, Rationally designed peptidomimetic modulators of Aβ toxicity in Alzheimer's disease, *Sci. Rep.*, 2015, **5**, 8139.
87 M. Algamal, J. Milojevic, N, Jafari, W. Zhang and G. Melacini, Mapping the interactions between the Alzheimer's Aβ-peptide and human serum albumin beyond domain resolution, *Biophys. J.*, 2013, **105**, 1700–1709.
88 D. D. Mruk and C. Y. Cheng, Enhanced chemiluminescence (ECL) for routine immunoblotting: an inexpensive alternative to commercially available kits, *Spermatogenesis*, 2011, **1**, 121–122.

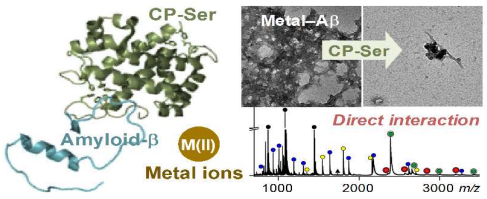

CP-Ser [S100A8(C42S)/S100A9(C3S) oligomer] interacts with metal-free and metal-bound $A\beta_{40}$ peptides and modulates their aggregation in the absence and presence of metal ions.